Engineering Structures 110 (2016) 48–58

Contents lists available at ScienceDirect

Engineering Structures

journal homepage: www.elsevier.com/locate/engstruct

Nonlinear instability analysis of long-span roofing structures: The case-study of Porta Susa railway-station

A. Carpinteri, F. Bazzucchi *, A. Manuello

Department of Structural, Geotechnical and Building Engineering, Politecnico di Torino, Corso Duca degli Abruzzi, 24, 10129 Torino, Italy

ARTICLE INFO

Article history:
Received 17 April 2015
Revised 16 November 2015
Accepted 19 November 2015
Available online 24 December 2015

Keywords:
Numerical analysis
Nonlinear instability analysis
Long-span roofing structures
Arch buckling
Porta Susa railway-station

ABSTRACT

Instability problems are going to be more and more important for long-span structures, especially for those where structural shape and loading capacity are strictly correlated. In view of this, a complete buckling analysis seems to be essential for the correct prediction of structural behaviour. At the same time, recent disasters, occurred in the last few years, such as the collapse of the new pavilion of Charles de Gaulle Airport in Paris (2006), have brought the instability of shallow long-span roofs at the cutting edge of structural engineering research. In this paper, different studies devoted to the stability of the large span roof of the new railway station of Porta Susa in Torino (Italy) are proposed. In particular, 2D models were realized in order to evaluate in-plane linear and nonlinear instabilities for different loading and restraining conditions of the steel arches constituting the bearing framework of the roof. These arches have been subdivided into different groups according to the geometric characteristics. It has been found that nonlinear analyses are able to give not only an interpretation of the post-buckling behaviour, but also a more correct evaluation of the safety factor for this kind of structures. Moreover, a parametric evaluation, taking into account different cross sections, is presented. The results reveal that much slender arches would offer the same safety factor as the existing ones due to the activation of a different resisting mechanism, although with an evident reduction in the employed material. Finally, the outcomes of this case-study could be generalized in order to investigate the behaviour of other structural typologies and to suggest alternative design approaches.

1. Introduction

The structural behaviour of long-span arches and roofs is a topic treated for a long time in structural engineering research [1–3]. For steel arches, several studies are related to their limit state design and to the consequent collapse mechanism: plastic collapse or buckling. Both the problems are usually studied through numerical approaches [4]. Plastic deformations occur rarely in slender structures where generally the buckling instability takes place when the material is still elastic. On the other hand, the influence of plasticity cannot be neglected in several cases, especially for arches subjected to large bending moments. By the limit analysis, closed form solutions have been obtained during the last sixty years [5]. Recently, the same problem has been analyzed for steel arches characterized by different sizes and shapes [6,7], and also, in very recent papers, for structures subjected to different restraining conditions and loading configurations [8,9]. It has long been recognized that a structure will in general lose its stability by either "snapping" or "buckling". From a theoretical point of view, the structure is said to snap when the equilibrium path emerging from the unloaded state loses its stability on yielding the first locally maximum value of the loading parameter; the structure is said to buckle when the path loses its stability at a point of bifurcation [10]. Physically, this means that when a snap-through instability occurs, the structure reach a new stable configuration when the maximum load is reached. On the opposite, this cannot happen after the attaining of the critical load of the classical buckling theory. As a consequence, not all the structural systems can have a snap-through instability, in fact it is possible only with some loading and geometric configurations. Generally, this problem regards shallow and slender compressed structures [10]. The in-plane elastic stability of arches has been analyzed for a long time since the usage of slender steel and pre-stressed concrete members has been intensified and the problem of buckling has become crucial [11]. In the last few years, different loading configurations and restraining conditions have been studied and many closed-form solutions have been obtained [12], included the case of shallow arches [13]. For elastically restrained arches, considering both geometric

* Corresponding author.
E-mail address: fabio.bazzucchi@polito.it (F. Bazzucchi).

http://dx.doi.org/10.1016/j.engstruct.2015.11.048
0141-0296/

and material nonlinearities, a closed-form solution has been recently proposed [14]. Generally, this problem is solved obtaining the critical load multipliers by the extraction of the eigenvalues of the arithmetic solving system associated with the linearized expressions of the total elastic potential of the structure; this means that the virtual work of each degree of freedom has to be stated. The so-called snap-trough instability phenomenon was analyzed in a series of works based on the analysis of simple structures [15,16]. The introduction of this different kind of instability has opened the way for the study of the post-buckling behaviour of structures by the analysis of the equilibrium paths [17,18]. Such problem is still actual and a more refined theoretical approach has been presented during the last twenty years [19]. The solution of this problem is completely different from the former one because the intrinsic geometrical non linearity makes impossible the expression of a linear arithmetic system. A numerical step-by-step approach is usually the most used and stable method, but many alternative ways has been proposed during the years, such as the power series expansions for the elastic potential used by Thompson [10]. For some structures, the instability problem could become of primary importance and then the post-buckling behaviour could be used as a leading design condition for structural optimization [20]. In addition, during the last 30 years, some experimental studies on the instability conditions of arches have been conducted [21].

However, the results of these general studies cannot entirely satisfy the safety needs in practical engineering. In fact, history teaches us that the most severe collapses of the past have generally occurred in extreme conditions [22] for which structural weakness emerged only after the failure, or, as in the case of terminal 2E of Charles de Gaulle airport, where the definitive failure cause has not been found yet.

Therefore, a complete and correct understanding of the structural stability response is necessary for the evaluation of the loading capacity of the entire building even in uncommon situations, i.e., for particular loading configurations, even when they are not prescribed by the codes.

The analysis, described in the present paper regards the structural behaviour of a series of arches that constitute the main steel skeleton of a large roofing structure, the actual core of the Porta Susa railway-station, built in Turin (Italy) in 2011 (see Fig. 1).

The numerical simulations that have been conducted in this investigation concerned: the load configurations, their effect and their possible mutual interaction in a geometrically nonlinear regime. This analysis appears to be able to identify the most vulnerable portion of the entire vaulted structure. Also the interaction between plastic collapse and buckling is analyzed and it is shown how the two mechanisms are strictly related and neither of them can be neglected in a correct evaluation of the safety factor.

The results outline the crucial role of the computational nonlinear analysis for the design of this kind of structures. In addition, a correct evaluation of the safety factor is obtained regarding the efficiency of the structural shape. Therefore, thanks to the study of the post-buckling, it has been possible to provide some preliminary remarks about the optimization process in the structural design. All the analyses that have been carried out showed that a true identification and comprehension of the collapse modalities leads to a more performing structural optimization regarding the restraining condition, the geometric configuration, and the mechanical parameters.

2. Analysis of the arch-type members

The structural members of the new Porta Susa station in Turin have been analyzed. These 108 unique (the geometry of each one is different to the other) arch-type members are composed of two equal straight columns and three upper circular arch portions (Fig. 2a and b). The employed section is the same for each element: an alveolar steel HEB 600 beam. Each frame is restricted by a pressed pivot-system at the basis of the columns. The procured rotational stiffness is in general not null, then the established constraint cannot be assumed only as a perfect hinge (see Fig. 2c). From this point of view, it must be considered the role played by the global rigidity to the structural instability, and especially how the collapse can be influenced by a certain restraining degree. For this reasons, the analyses conducted in the present paper will be carried out taking into account the two extreme restraining conditions: (i) perfect hinges and (ii) fully fixed supports. Operating this way, those two conditions will envelope all the possible intermediate circumstances. Obviously, these considerations are necessary in a second-order analysis, because in the presence of a geometric nonlinearity an higher restraining degree not always guarantees a greater maximum critical load or a softer post-peak branch. The two modelling condition has been adopted in all the analyses in order to make comparison between them.

Eventually, the structure of each arch frame member is longitudinally connected by a set of straight beams laying at the top of each frame and by a complex bracing system (see Fig. 2d). Furthermore, some additional transversal elements offer a support to pedestrian platforms, stairways, elevators and anchorages of the tunnel. All these elements, due to their reduced contribution to the roof in-plane stability, were neglected in the numerical simulations proposed in the next sections. The lack of a rigid connection with the vertical elements and the reduced flexural inertia of the longitudinal elements, in comparison to the one of the arch frames, makes this as a right assumption. In the present paper, a classification has been proposed according to the following geometrical parameters: $OR = l_s/l_i$ and $SR = l_s/f$, that define the Opening Ratio and the Shallowness Ratio of each arch frame as shown in Fig. 2b. *OR* remains approximately constant around the unitary value, whereas *SR* shows a wide variation from a minimum value equal to 2.62 for the least shallow arch frame to a maximum value of 11.03 for the most shallow one. By means of an unitary step variation of *SR*, ten sets of arch frames have been identified and for each set the arch frame with minimum *SR* value has been selected as the representative one (Fig. 3). Operating this way, each typical arch frame differs from the nearest two by a variation in *SR* at least equal to 1. The most shallow one has been chosen because it represents the most severe geometric configuration towards the snap-through instability. All the numerical analyses have been implemented in the finite element solver and modeller LUSAS 14.3. For the nonlinear analyses, a co-rotational formulation together with an arc-length based solver algorithm has been used. In this way, the post-peak paths can be followed, and if an incremental displacement parameter is performed, even the unstable branch can be carried out by the solver.

3. First-order analysis

As a first stage, for each representative arch frame the Eulerian buckling load, by the critical multiplier λ, has been evaluated according to the following structural constraint conditions: double hinged and fully restrained arches. At the same time, two different loading configurations (1 and 2), assumed according to the Eurocode recommendations [23–25], and two additional ones (locally distributed, 3 and 4) were imposed to evaluate the buckling effects as shown, for the double hinged arch, in Fig. 4. Every load configuration has the same linear density and its position on the span is representative for a particular external loading configuration. Together with the classical load applications (1 and 2), Configura-

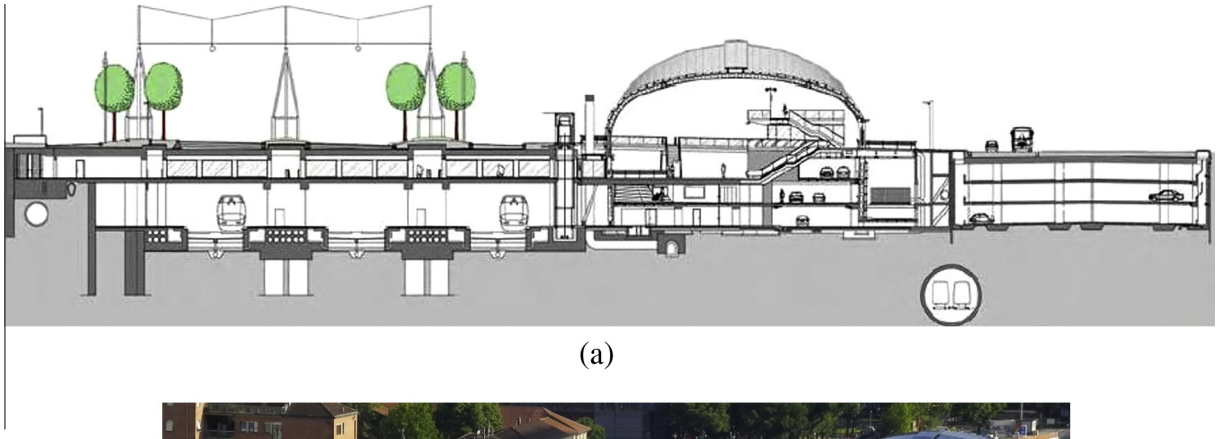

(a)

(b)

Fig. 1. Cross-section of the Railways station (a). Picture of the external roof (b). The Railway station was built in 2009.

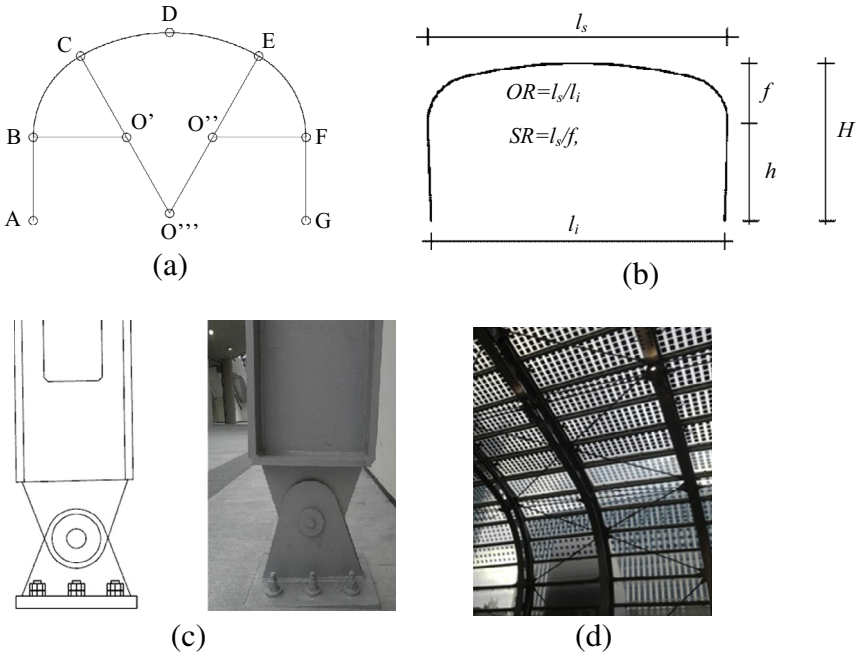

Fig. 2. The arch-type frames are composed by two equal vertical straight columns and three upper circular arch portions (a) and (b). Base connection (c) and a detail of the longitudinal bracing system (d).

tion 3 and 4 simulate some supplementary and eventual external load positions along the span. For the double hinged arch configuration, the results regarding the λ multiplier of the four adopted loading schemes are reported in Fig. 5a. The multiplier value reached a minimum value equal to 26.7 for *ARCH 8* (which for simplicity stands for the arch frame number 8) with a load configuration characterized by a uniformly distributed load (Loading Configuration 1). This means that this particular structural

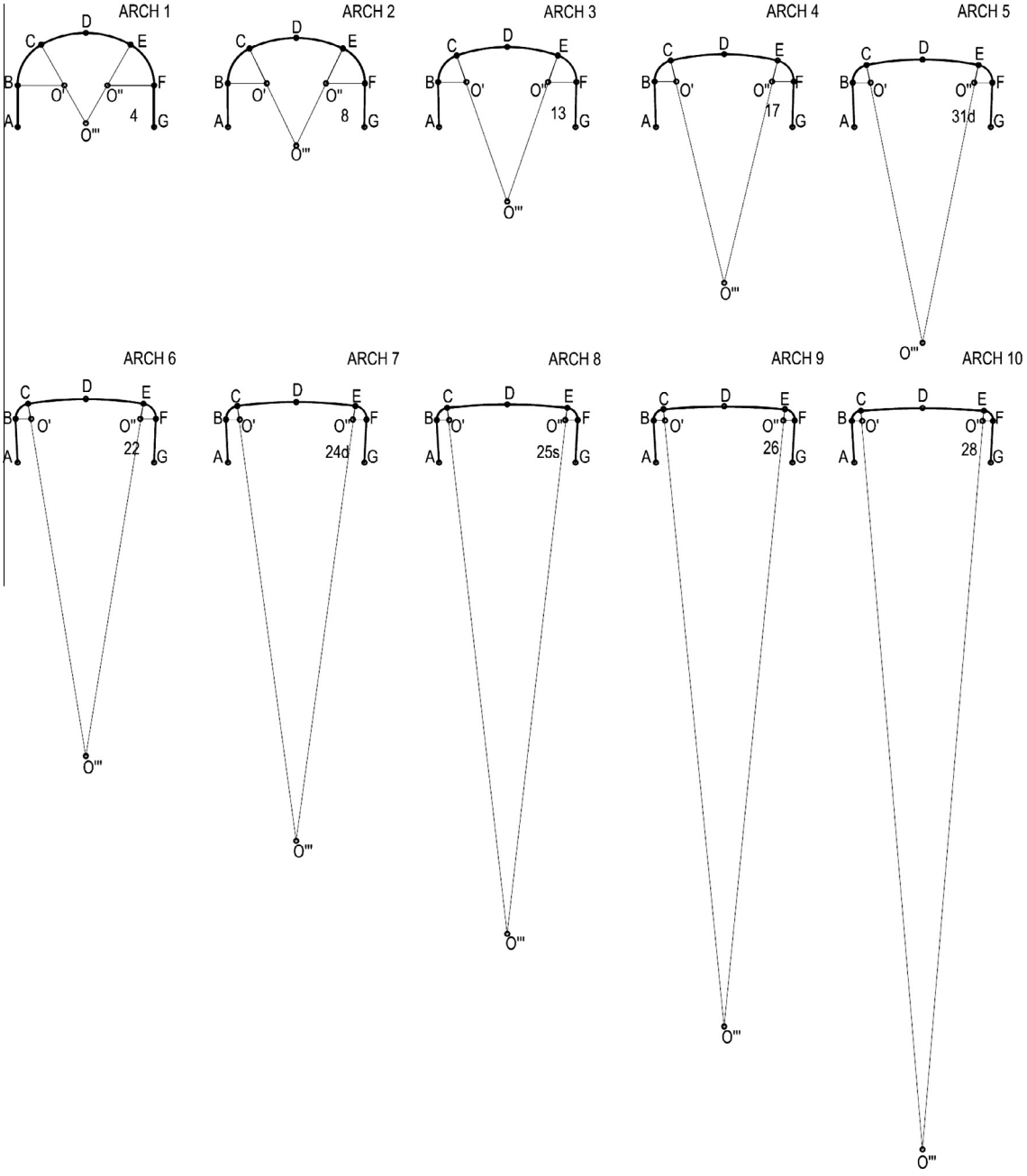

Fig. 3. Ten sets of arches are identified. For each one a representative arch has been chosen for the numerical analysis.

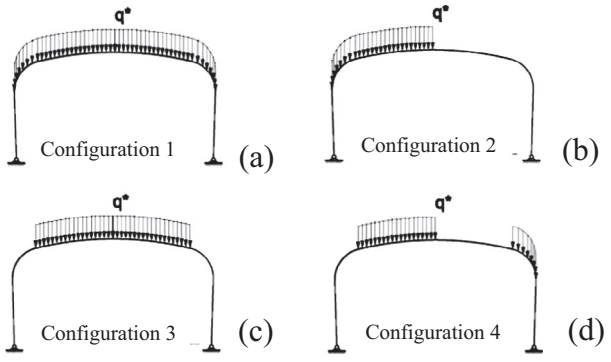

Fig. 4. The four configuration of the loading conditions in the case of hinged arches.

arrangement, as a combination of geometry, constraints and loads, is the most sensitive to buckling. In particular, the geometry of the *ARCH 8* creates the minor rigidity condition towards the applied loading and then the critical multiplier results as the lowest one. A more shallow structure procures an additional strength as can be seen by the higher value of λ for *ARCHES 9* and *10*. This contribution has to be also associated with the curvature near the top of the column, which confers a supplementary local stiffness. Furthermore, the loading Configuration 1 appears as the heaviest condition for each arch frame with a small variation of the critical load factor. At the same time, the non symmetric configurations seem to be the less burdensome for all the arch frames, especially for those characterized by mid values of SR. These variation of the λ factor for the considered configurations can be justified by the same explanation given for the lower value of the *ARCH 8* in the load Configuration 1.

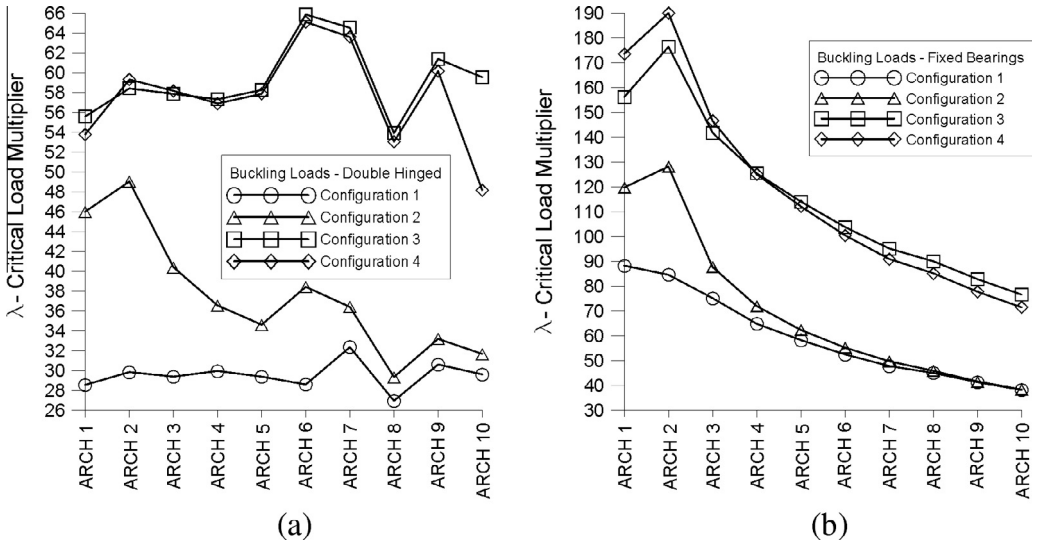

Fig. 5. Multiplier factor for each arch types in the case of double hinged (a) and fully restrained (fixed bearing) members (b).

In Fig. 5b, the results for the fully restrained condition are reported for the same loading Configurations 1–4. First of all, it is possible to observe how each value of the critical multiplier is larger than the previous ones and the Load Configuration 1 is again the most unsafe. The results confirms that, as expected from a linear analysis, the greater the rigidity of the constraint, the higher is the load multiplier. Even in this case, the non symmetric loading seems to lead to a more stable condition for the structure. It is worth to note, that in this particular restraining condition, the geometry of *ARCH 2* results as the most efficient one towards Load Configurations 2, 3 and 4. Furthermore, the presence of fixed bearings tend to uniform the values of the buckling loads, especially for the shallower members. This particular behaviour will be confirmed in the further analyses, but it has to be ascribed to the combination of high structural rigidity and high shallowness ratio. In addition, it can be observed that the buckling load diminishes with the increase in the *SR* factor. At the same time, the higher is the constraint degree, the lower the dependency of λ on the *SR* ratio (especially for higher *SR* ratios).

At the end, a comparison between theoretical buckling load of circular arches with the same span subjected to a uniformly distributed load [1] and the steel members adopted in the case-study, showed noticeable differences (Fig. 6): for each arch member, the numerically computed buckling load is lower than the one theoretically evaluated for the respective circular arch. Therefore, the structural behaviour of the considered structure is very far from the one of an actual arch. These first results show that the presence of the columns leads the structure to a less efficient shape with regard to stability. This evidence will be confirmed in the nonlinear analysis, reported in the next section.

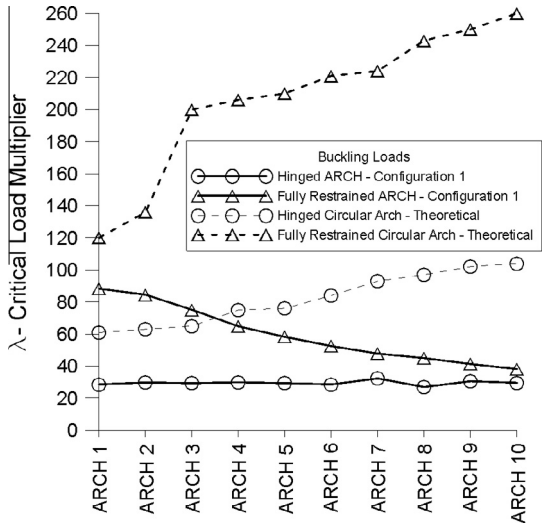

Fig. 6. Multiplier factor of Load Configuration 1 for each arch types in the case of double hinged and fully restrained (fixed bearing) members compared to theoretical buckling loads of circular arches subjected to uniformly distributed loads.

4. Second-order analysis

The second kind of analyses were conducted imposing an incremental vertical displacement *d* to the top of the arches and extracting the value of the vertical reaction *F* at the same node. By working on these parameters, it is possible to obtain the *F* versus *d* curve for each arch, which describes the structural response accounting for geometric nonlinearity. No external loading are applied to the structure, then the equilibrium path has to be associated to the sole application of the displacement *d*.

Using such numerical simulation, it is also possible to evaluate the unstable equilibrium path beyond the maximum load according to a post-buckling analysis. Both of the two previous restraining conditions (fully restrained arch and double hinged arch) were considered, and, for the numerical models, the nonlinear thick beam elements have been used along with an updated co-rotational formulation for the solving equation system. Each displacement increment was assumed equal to 0.025% of the maximum displacement adopted, which coincides with ¼ of the total height of each arch frame.

In Fig. 7, the *F* versus *d* curves for the hinged arch condition have been reported. It can be noted the presence of a sharp transition in the structural behaviour between the first three arches (*ARCHES 1–3*), which are the less shallow, and the remaining ones.

ARCHES 4–10, in fact, reached the maximum load in correspondence to a displacement range between 2 and 3.5 m, and after this phase the equilibrium path proceeds with a softening post-buckling behaviour. On the contrary, for the first three arches, even with the achievement of very large deformations ($d \geqslant ¼H$) the maximum load seems not to be reached. According to the definition of the *SR* parameter, a particular value can then be obtained

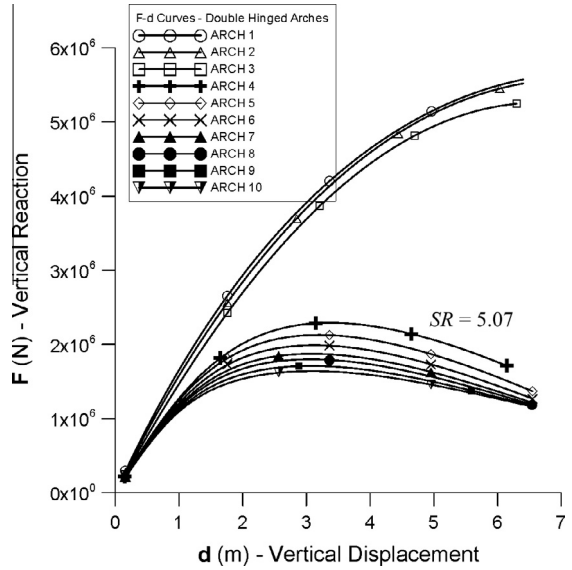

Fig. 7. *F–d* curves related to ARCHES 1–10 considering a double hinged restrain conditions. A SR value equal to 5.07 may be assumed to recognize the transition between the two kinds of equilibrium paths.

to describe the transition in the behaviour of the two arch sets: *ARCHES 1–3* and *ARCHES 4–10*. In the case of the arches reported in Fig. 7, the transition is at an *SR* value equal to 5.07 (*ARCH 4*).

As is well known [8], the decrease in the height of the arch generally leads the structure to the secondary type of progressive instability, that is the one characterized by an immediate softening post-peak branch. According to this fact, lower values for the buckling loads were obtained by using a nonlinear analysis, which interprets correctly these kind of instabilities, with respect to the results that came out from linear computations.

Fig. 8 shows *F* versus *d* curves of the arches with fixed supports at the basis of each column. If compared to the previous case (Fig. 7), the reduction in the bearing capacity takes place with a gradual transition for all the elements. At the end of the loading

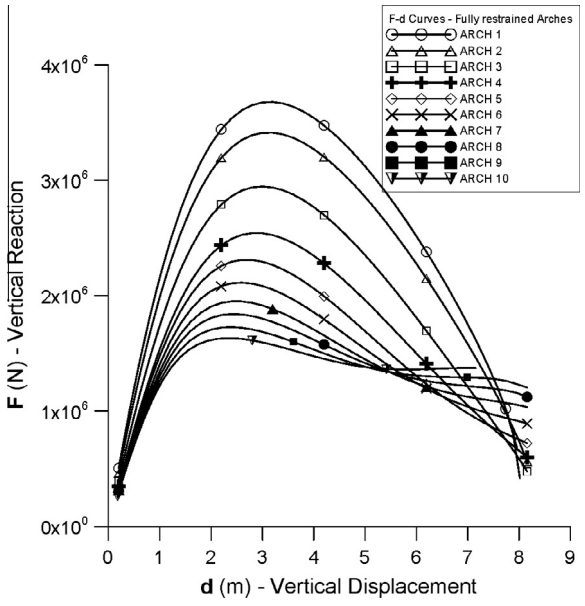

Fig. 8. *F–d* curves related to ARCHES 1–10 considering a fully fixed restrain conditions. Resultant equilibrium paths show no transition on the structural behaviour.

process, each arch has reached the peak condition and the equilibrium path presents a different behaviour along with the decrease in the SR parameter. *ARCH 10*, which is the most shallow one, shows in fact a tendency to a snap-through instability in the last branch of the post-buckling path.

As a limit case, the behaviour of a portal frame (an arch with $SR \to \infty$, Fig. 9) was analyzed: the *F* versus *d* curves of the portal for the two already used restraining conditions were overlapped to the curves of the ten arches. In an unexpected way, the curves of the portal configurations lay in the transition zone. This can be easily observed in Fig. 9a (double hinged arch configuration), where it is possible to conclude that there is a limit value *SR* for which it is not advantageous, in structural stability terms, to use a curved structure; this is due to the fact that the contribution of the shape is not effective to the resistance because the generated internal axial forces become larger in the horizontal direction. In a portal frame this cannot happen since there are no such components because the vertical displacement applied on the mid section of the horizontal beam produces axial forces only on the columns. This condition induces the opening of the columns and the consequent collapse condition. The *SR* limit ($SR = 5.07$) defines the value for which *ARCH 4*, and the consecutive ones up to *ARCH 10*, show a behaviour much more similar to that of a portal frame than to that of an actual curved arch.

Eventually, the values of the buckling loads related to the different order analyses in the two examined restraining conditions were reported in Table 1 and in Fig. 10. In order to perform this comparison, the first-order linear analysis was implemented assuming a loading condition characterized by a concentrated vertical force at the crown of each arch. This condition is indeed the dual one to the incremental displacement analysis, which in fact measures the vertical reaction at the top of the crown of each arch.

As reported in Fig. 10a, only in the case of hinged arches it is possible to recognize for the first three arches that the second-order analysis leads to higher values of the buckling load. This results can be interpreted considering that less shallow arches are generally affected by a first kind instability which is not characterized by any progressive effects. Only in these cases, in fact, a first-order analysis results to be more safe in terms of capacity design. In all the other instances the nonlinear analysis involves lower buckling loads with a proportional factor ($F_C^{I\ order}/F_C^{II\ order}$) equal to 2 or 4 for double hinged arches or fully restrained arches, respectively (see Table 1).

A further remark can be done considering that with the linear analysis, the fully restrained arches show always larger values of the critical load with respect to the hinged ones; using a second-order analysis, it is possible to observe that these results are true only for the most shallow arches. This is another disadvantage of the usage of a first-order analysis, that generally associates more stability to more restrained conditions. As far as the second-order nonlinear analysis is concerned, the evaluation of the equilibrium condition in the progressive deformed configuration was taken into account. Moreover, comparing the two deformed structures obtained in the two analyses, it can be seen that the one related to the linear procedure (Fig. 11a) is not consistent with the last considered loading configuration, which is characterized by the concentrated load at the crown. The second one (Fig. 11b), related to a vertical incremental displacement at the crown of the arch, corresponds to the actual loading process.

5. Influence of the load configuration

In order to determine the effects of the loads on the stability of the considered structure, the previous nonlinear analysis will be now conducted with the presence of two different load configura-

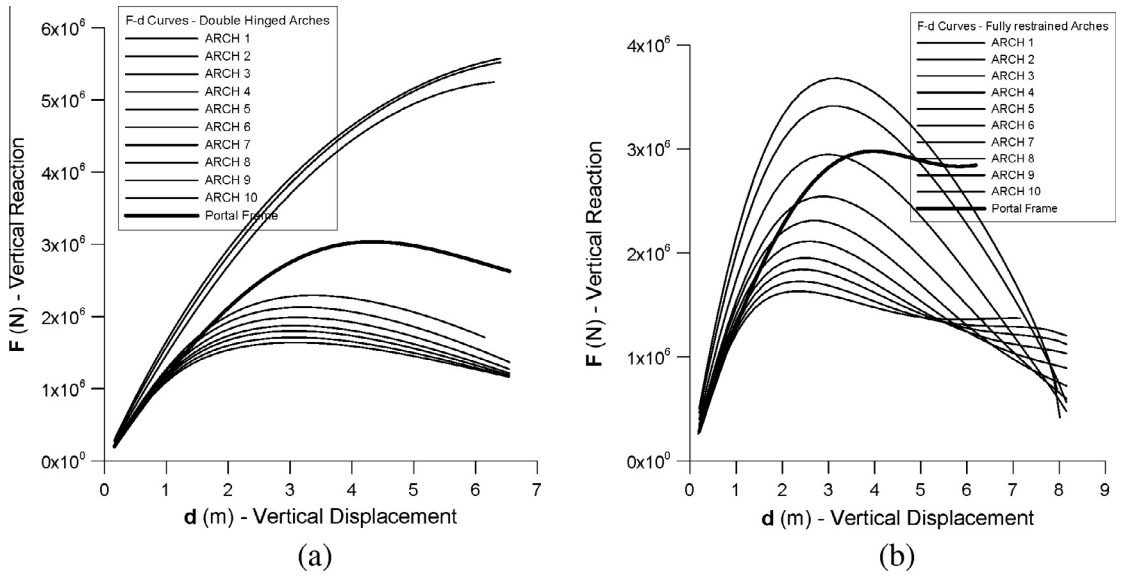

Fig. 9. *F–d* curves of a portal for the two restrain conditions, double hinged (a) and fully restrained (b), are overlapped to the curves of the ten arches.

Table 1
Comparison between the maximum buckling loads obtained by first and second order analysis of the arches. Fully restrained and double hinged conditions.

	Fixed bearings		$F_C^{I\ order}/F_C^{II\ order}$	Double hinged		$F_C^{I\ order}/F_C^{II\ order}$
	$F_C^{I\ order}$ (kN)	$F_C^{II\ order}$ (kN)		$F_C^{I\ order}$ (kN)	$F_C^{II\ order}$ (kN)	
ARCH 1	11526.0	3678.5	3.1	4053.0	5574.5	0.7
ARCH 2	11328.1	3412.1	3.3	4360.1	5519.2	0.8
ARCH 3	11091.9	2946.0	3.8	4321.4	5254.0	0.8
ARCH 4	10237.4	2542.2	4.0	4373.7	2291.8	1.9
ARCH 5	9438.6	2309.8	4.1	4504.5	2128.5	2.1
ARCH 6	8409.1	2112.9	4.0	4886.9	1988.8	2.5
ARCH 7	7461.9	1951.2	3.8	4418.0	1874.0	2.4
ARCH 8	6864.6	1840.7	3.7	4156.3	1799.3	2.3
ARCH 9	6292.1	1727.8	3.6	3968.4	1710.5	2.3
ARCH 10	5446.7	1640.7	3.3	3703.6	1631.6	2.3

tions. These conditions represent respectively the existence of a symmetric and a non symmetric distributed load, applied statically to the structure, on the upper portion of the arches. According to these loading configurations, the *F* versus *d* curves were obtained considering the two previous different restraining conditions (Fig. 12).

In Fig. 13, the resultant instability behaviour for *ARCH 1* was reported and it can be observed how only the double hinged arch condition (Configurations 1–3) is influenced by the external loads. Therefore, the non symmetric load (Configuration 3) comes out with a drastic reduction in the structural resistance. This serious abatement in the buckling load induces a catastrophic collapse of the arch with serious lateral deformations and loss of the bearing capacity (softening branch). The three overlapped curves (configurations 4–6) correspond to the fully restrained arch condition and it can be seen that in these cases the buckling load and the behaviour are not influenced by any of the external loads. This happens because the redistribution of internal stresses and forces allows the structure to explicate the same vertical reaction at the crown for every loading configuration. On the one hand, as can be observed, the fixed restraining condition induces the arch to behave as a portal frame subjected to vertical load. In this case, no increments in axial stresses can be generated and the horizontal beam does not reach compressive buckling. On the other hand, the double hinged arch case is characterized by additional rotations at the basis, then the consequent deformations cannot be compensated and a progressive instability condition is achieved as the loading process moves forward.

Also in the case of *ARCH 2*, it is possible to observe that the double hinged arch condition is affected by the presence of additional external static loads (see Fig. 14). In this case, both the loading configurations lead to a progressive instability with a consistent reduction in the buckling load (compare Configurations 2 and 3 with configuration 1 in Fig. 14). Observing now the *F* versus *d* curves relatively to *ARCH 3* (Fig. 15), it can be pointed out that the post-critical behaviour of the structure takes place sharply with the non symmetric load configuration in the double hinged condition. In this case, a snap-back instability appears (Configuration 3) proving that on these conditions an high structural sensitivity is present. This is a particular snap-through instability, that happens in fact with a regression of the total displacements after the attaining of the maximum load (post-peak softening branch is characterized by a positive slope). At the same time, taking into account that the numerical analyses are controlled by the displacement, it is possible to understand why this branch became evident. In a real loading process, the snap-through will occur with a sharp decrease of the bearable loading and no displacement. In this way, the structural collapse can be considered very drastic.

The curves analyzed so far are related to the tallest arches (*ARCHES 1–3*), which previously indicated a behaviour close to that of circular arches. A simple nonlinear analysis (without the presence of external distributed loads) outlined the nature of the buck-

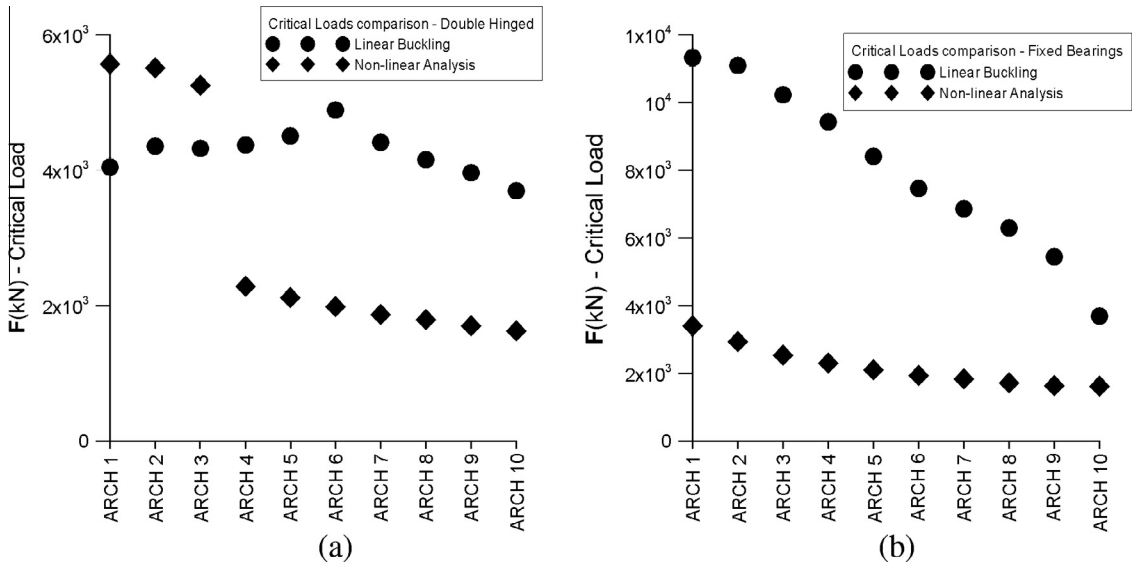

Fig. 10. Comparison of the values for the buckling loads between the different order analysis for the two restraining conditions: Fully restrained (a) and double hinged conditions (b).

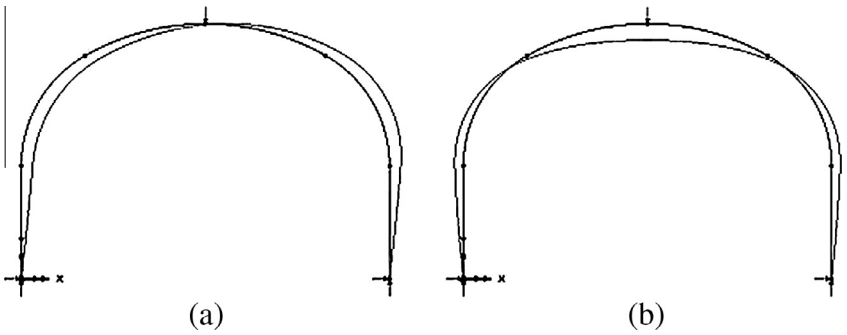

Fig. 11. Comparison between the deformed structure after a linear buckling analysis (a) and a second order numerical computation (b) with the same loading configuration (central concentrated force on the top of the arch).

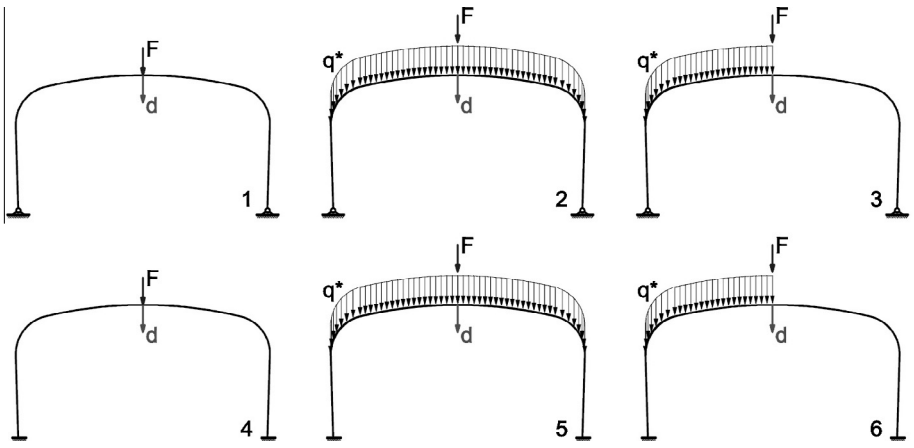

Fig. 12. Loading configurations and restraining conditions used in the numerical simulations.

ling that was a first-kind one, with no progressive phenomena and characterized by an high maximum load (Section 4, F versus d curves, Configuration 1). Only by the investigation of the interaction between different loading configurations pointed out how much those structures suffer the instability and how the post-critical behaviour is affected by this: the obtained curves represents the equilibrium path under the external loading configuration and taking into account the intrinsic geometric nonlinearity. A linear buckling analysis is no sufficient to the correct evaluation of the critical load, and even the extraction of a general equilibrium path needs a detailed analysis arrangement to be a proper usable tool.

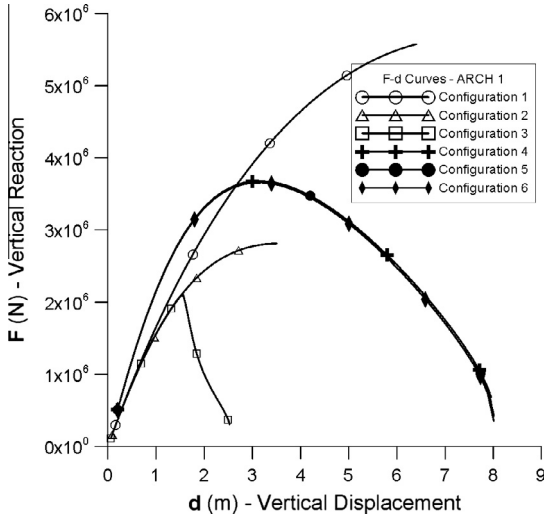

Fig. 13. Influence of the loading configuration on *F–d* curves for ARCH 1.

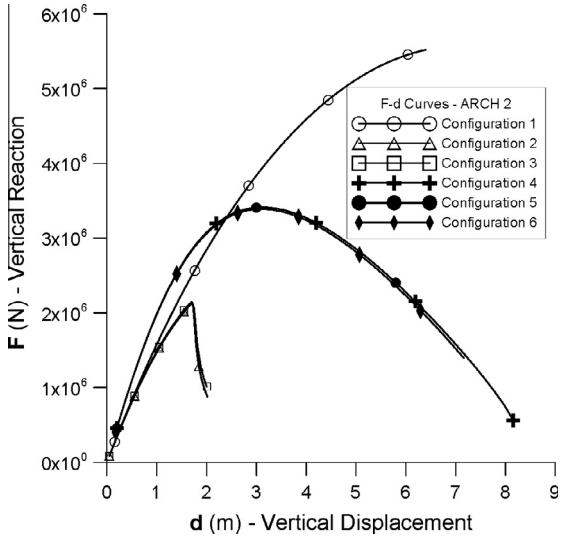

Fig. 14. Influence of the loading configuration on *F–d* curves for ARCH 2.

Eventually, the *F* versus *d* curve of *ARCH 4* is reported (Fig. 16). It can be observed that the additional distributed loads are not influencing the stability of the structure. As in the previous cases, this is due to the fact that *ARCHES 4–10* behave like portal frames. The curves for these arches are rather similar to those obtained in the case of portal frames (see Fig. 9).

For *ARCH 10*, which is the most shallow, the overlapping of the six curves (related to Configurations 1–6) appears proving how this behaviour is very close to that of a portal frame. The latter in fact has a unique in-plane structural stability response (*F* versus *d* curve), which is not influenced by any additional vertical loads configuration. The presence of external loads on the horizontal beams can in fact only interfere with the vertical displacement since the vertical columns will absorb the load step by step by an increasing of their axial force. According to the particular implemented analysis, the vertical displacements are imposed then the resultant equilibrium path will be no influenced by the application of superposed vertical loads. Obviously, this happens because a snap-through cannot occur for such structural arrangement and then every point of the equilibrium path is a stable one.

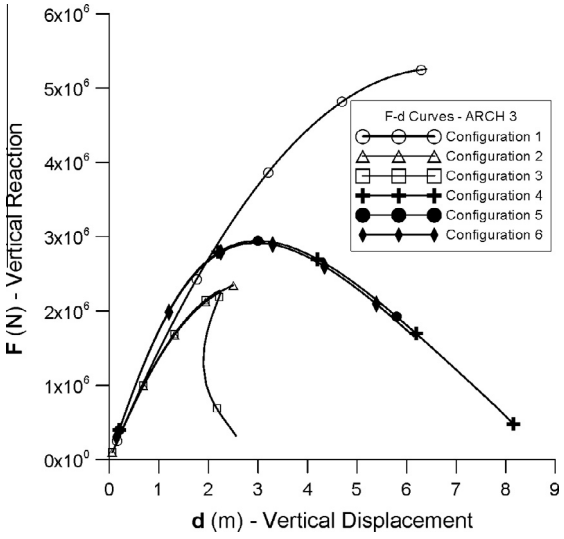

Fig. 15. Influence of the loading configuration on *F–d* curves for ARCH 3. Snap-back instability.

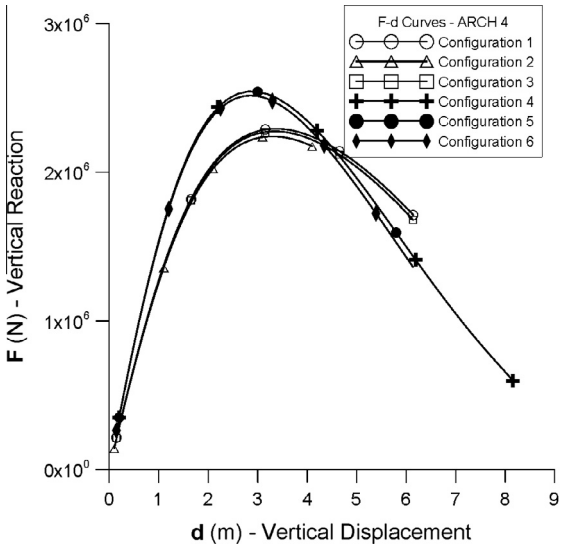

Fig. 16. Influence of the loading configuration on *F–d* curves for ARCH 4.

6. Influence of plasticity

It is worth to note that the steel arches were analyzed assuming a linear elastic constitutive law. Nevertheless, a plastic collapse investigation is necessary in order to determine the actual failure mechanism. A plastic analysis was conducted on *ARCH 1*, and *ARCH 10*, respectively the tallest and the most shallow, by an incremental loading routine in the simulation and considering the two different previous configurations concerning the external loads. For the restraining system at the foundation, two hinges were used in order to minimize the possible redistribution of the internal stresses. The maximum resisting bending moment was estimated to be equal to 1.47×10^3 kN m, and when the arch reaches it in one of its sections, the first critical plasticity load is evaluated. For both the analyzed arches, the most severe load configuration is the one with the vertical uniformly distributed load along the entire span. For *ARCH 1*, the collapse condition is reached with the formation of a plastic hinge at point D (Fig. 2) and progressively at the top of the columns, identifying the critical load by a multiplier factor λ_{PLA}

equal to 15. Recalling the multiplier associated to pure instability, $\lambda_{BUCK} = 28.5$, obtained in the section on linear buckling analysis, it is to be noted that the latter is almost twice as much as the one related to plasticity. Yielding then occurs before buckling, confirming the high sensitivity of the structure to this kind of collapse. The last evidence may be associated to the section and material properties. Even if the results seem to exclude instability phenomena in favour of plastic collapse, considering both geometrical and material nonlinearities, the multiplier λ becomes equal to 9.5. It is evident that neglecting the instability effects ($\lambda_{PLA} = 15$) leads to overestimate the maximum load by 50% with respect to the true one (9.5). It is worth to note that it is possible to obtain similar results for the multiplier λ by using the Merchant–Rankine formula:

$$\lambda = \lambda_{PLA} \frac{1}{0.9 + \frac{\lambda_{PLA}}{\lambda_{BUCK}}} = 9.83 \quad (1)$$

The analysis can be repeated for *ARCH 10* and the value of the plasticity multiplier λ_{PLA} results to be equal to 10. The collapse mechanism is now different, with the top of the columns reaching first the plastic bending moment. Comparing this value with that obtained by the instability analysis, namely 29.6, it can be observed how the latter collapse does not prevail. Nevertheless, an inelastic incremental analysis leads to a value of the multiplier λ equal to 7.1, confirming once again an abatement of about 1/3 of the plastic load multiplier. Also in this case, the previous formula leads to a similar value:

$$\lambda = \lambda_{PLA} \frac{1}{0.9 + \frac{\lambda_{PLA}}{\lambda_{BUCK}}} = 7.47 \quad (2)$$

In conclusion, nonlinear buckling analyses have to be conducted for the correct estimation of the safety factor.

7. Minimum section calculation and structural optimization

Purpose of the following analysis is to study how the progressive instability phenomena are affected by a variation in the inertia of the beam cross section. The arch chosen for the analysis is *ARCH 3*, the one that in the previous analyses showed a snap-back in correspondence of a non symmetric loading configuration. *F* versus *d* curves were obtained considering different cross sections, characterized by a uniform decrease in the section depth, from HEB 600 to HEB 200. For all the analyzed sections (S1–S7), the same alveolar holes in the same proportion with the original one were maintained. In Table 2, the properties of each adopted section are reported.

Observing the *F* versus *d* curves (Fig. 17), it can be noted that the snap-back phenomenon persists as a post-critical behaviour for all the sections except for the last one (Section 7 in Table 2). In the particular non symmetric load configuration, only the geometry of the frame influences the structural response of the arch frame. Also for S6, which has a moment of inertia equal to 15% of the original one, a small snap-back after the peak load takes place. This

Table 2
Geometrical properties of the sections adopted in the simulation.

	Section	h (mm)	A (mm^2)	A/A_1	I_y (mm^2)	I_y/I_{y1}
HE 600B	1	600	22,350		1,675,125,000	
HE 550B	2	550	21,285	0.95	1,341,003,906	0.80
HE 500B	3	500	20,235	0.91	1,053,119,792	0.63
HE 450B	4	450	18,650	0.83	785,610,938	0.47
HE 400B	5	400	17,080	0.76	567,800,000	0.34
HE 300B	6	300	13,260	0.59	248,606,250	0.15
HE 200B	7	200	6910	0.31	56,210,000	0.03

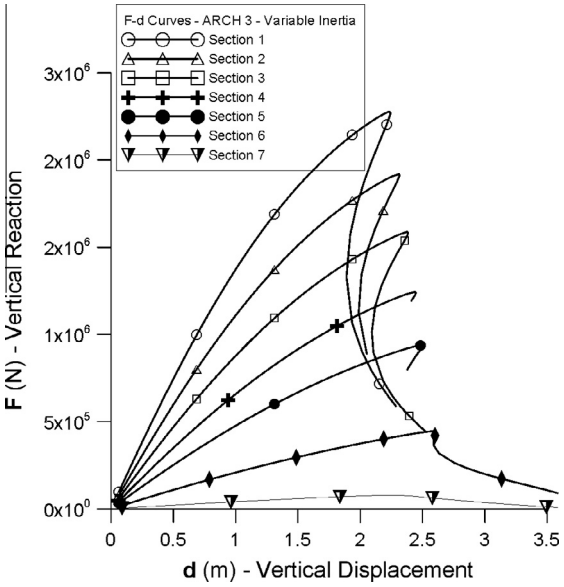

Fig. 17. *F–d* curves for ARCH 3 using different section with decreasing inertia.

means that, the geometric configuration, or in other words, the *form*, in the key factor which influences the most the structural instability behaviour.

By these analyses, it is possible to point out additional considerations about the role played by the global rigidity. When the structure is rather flexible, yielding becomes almost non influential about the collapse condition. Due to the high deformability of the structure, buckling becomes the primary collapse condition. The evaluation of the critical load in this condition can be improved by a sole incremental analysis in the linear elastic regime (Fig. 15). Accordingly to the previous analysis, the value of the multiplier λ for *ARCH 3* with the original section (S1) is equal to 9.7. It is worth to note that almost the same value can be obtained by using S5 (see Table 2). Recalling in fact the multiplier $\lambda_{BUCK} = 28.5$, obtained in the linear elastic regime by a first-order analysis as a safety factor, and associating it to the first curve in Fig. 17, the abatement of the critical load going through the *F* versus *d* curves S1 to S5 is equal to almost 1/3. This result shows that the utilization of rigid and massive cross sections, when instability, and its interactions, cannot be neglected, not always leads to a superior safety level. Indeed, the same structural performances, in terms of critical multiplier, can be obtained with a cross section that, recalling Table 2, allows a saving close to 25% of the employed material. This means that, operating on the structural form it is possible to modify the collapse mechanisms of a structural arrangement. This could be very important when the system has multiple failure possibilities, such as the one analyzed in this paper. Excluding in fact a collapse mechanism means also to avoid his possible interaction with the ones that persist. The example reported, shows that excluding the material yielding by the utilization of a lighter and more deformable structure the structural behaviour is all influenced by the instability, in particular the snap-through one. Obviously, the global project could be affected by many other design problems, but the objective of this analyses is to show in detail how a direct structural optimization is possible to be carried out if the instability problem is extensively studied.

8. Conclusions

In the present study, different kinds of numerical analysis have been conducted in order to evaluate, by an innovative approach,

the possible optimization of long-span roofs. In particular, first-order analyses, second-order analyses, and the effects of the load configuration together with those of the plastic behaviour have been taken into account in the numerical simulation of the roofing structures of Porta Susa Railway station, built in Turin in 2011. From the simulations and their results, a structural optimization can be obtained using the buckling condition as a guideline for structural design. First of all, ten representative arches of the station have been selected as the object of the numerical analysis by subdividing the steel framework in sets according to different geometrical parameters. For each arch, a linear buckling analysis has been performed and the critical multiplier λ has been evaluated in four different loading configurations and two different restraining conditions. The simulations pointed out that the double hinged arch condition is always characterized by lower values of critical loads with respect to the fully restrained one. It has been also possible to demonstrate that the uniformly distributed load configuration is the most dangerous. Furthermore, a comparison with the theoretical buckling load of actual circular arches showed that the values of λ are very different to the ones of the steel framework with the same span.

In addition, a comparison with the theoretical buckling load of circular arches showed that the values of λ are very different to the respective ones of the roofing structure analyzed.

As a second approach, a nonlinear incremental analysis has been conducted for the same ten arches with the two previous restraining conditions. The numerical results show that in the case of double hinged arch condition a sharp transition of the structural behaviour is present. The three least shallow arches, in fact, did not reach a peak value of the load for the imposed displacements. The other ones, instead, show a softening branch of the equilibrium path after the achievement of the maximum load. Operating in this way, a nonlinear analysis for a portal frame proved that the most shallow arches are less effective than this last structure in terms of stability. Lastly, a comparison with the critical loads obtained by the linear analysis evidenced that, excluding the three tallest arches in the double hinged arch condition, the maximum load obtained with the second-order simulation is always lower. This means that, performing only a linear buckling analysis, the safety factor of the structure is generally overestimated. Furthermore, the influence of the load configuration along the span has been investigated and the results have pointed out that, for the first three arches, the non symmetric configuration is the most severe. This loading process in fact leads to lower values of the maximum load and to a worst post-buckling behaviour; *ARCH 3* is characterized even by a snap-back branch.

Linear buckling analysis does not permit to put this phenomenon into evidence. It also considers the non symmetric loading configuration characterized by an higher value of the critical load multiplier with respect to the case of uniformly distributed load. The influence of the load configuration becomes less important if the restraining degree is higher or if the arch is more shallow. These results confirm the behaviour of the arches to be similar to that of portal frames.

Plasticity influence has been also taken into account by performing a both geometrically and physically nonlinear analysis for the least and the most shallow arches. It is demonstrated that plasticity is the primary collapse mechanism for the arches of the steel framework of the station. Nevertheless, if the instability effect is neglected in the analysis, the peak load results overestimated by almost 50%. This last simulation proved once again the importance of performing a nonlinear instability analysis even for structures that seem to be less sensitive to buckling than to yielding.

As a final consideration, a structural optimization has been conducted implementing a nonlinear analysis with variable inertia of the beam cross sections. The arch that has been selected is the one characterized by the worst post-buckling behaviour: *ARCH 3* with a non symmetric load configuration. Such analysis evidences that, using smaller sections for the steel framework, the same maximum bearable load as that of the larger original ones could be reached; this is possible because plasticity effects become less critical for slender structures. Using then the instability condition as the key design factor, a saving of 25% of the material could be possible for the steel members of the roofing.

Acknowledgements

Special thanks are due to AREP society in the person of Arch. Salvatore D'Ascià for the collaboration. In addition, the authors are also very grateful to Eng. C. Piantino and Eng. E. Matta (of SI. ME.TE S.r.l.) for the supply of the executive version of the Porta Susa Railway Station structural drawings and for the courteousness of sharing the design information.

References

[1] Timoshenko S, Gere JM. Theory of elastic stability. New York: McGraw-Hill Co., Inc.; 1961.
[2] Dickie JF, Broughton P. Stability criteria for shallow arches. J Eng Mech Div ASCE 1971;97(EM3):951–65.
[3] Gjelsvik A, Bodner SR. Energy criterion and snap-through buckling of arches. J Eng Mech Div ASCE 1962;88(EM5):87–134.
[4] Calhoun PR, DaDeppo DA. Nonlinear finite element analysis of clamped arches. J Struct Eng ASCE 1983;109(3):599–612.
[5] Onat ET, Prager W. Limit analysis of arches. J Mech Phys Solids 1953;1:77–89.
[6] Pi Yong-Lin, Trahair NS. Non-linear buckling and postbuckling of elastic arches. Eng Struct 1998;20(7):571–9.
[7] Pi Yong-Lin, Bradford MA. Non-linear in-plane postbuckling of arches with rotational end restraints under uniform radial loading. Int J Non-Linear Mech 2009;44:975–89.
[8] Pi Yong-Lin, Bradford MA, Uy B. In-plane stability of arches. Int J Solids Struct 2002;39:105–25.
[9] Bradford MA, Pi Yong-Lin, Uy B. In-plane elastic stability of arches under a central concentrated load. J Eng Mech 2002;128:710–9.
[10] Thompson JMT. Basic principles in the general theory of elastic stability. J Mech Phys Solids 1963;11:13–20.
[11] Austin WJ. In-plane bending and buckling of arches. J Struct Div, ASCE 1971;97 (ST5).
[12] Pi Yong-Lin, Bradford MA, Tin-Loi F. Non-linear in-plane buckling of rotationally restrained shallow arches under a central concentrated load. Int J Non-Linear Mech 2008;33:1–17.
[13] Pi Yong-Lin, Bradford MA, Tin-Loi F. Non-linear analysis and buckling of elastically supported circular shallow arches. Int J Solid Struct 2007;44:2401–25.
[14] Pi Yong-Lin, Bradford MA, Tin-Loi F, Gilbert RI. Geometric and material nonlinear analysis of elastically restrained arches. Eng Struct 2007;29:283–95.
[15] Huang NC, Vahidi B. Snap-through buckling of two simple structures. Int J Non-Linear Mech 1971;6:295–310.
[16] Bellini PX. The concept of snap-buckling illustrated by a simple model. Int J Non Linear Mech 1972;7(6):643–50.
[17] Chajes A. Post-buckling. J Struct Eng, ASCE 1983;109(10):2450–62.
[18] Bellini PX, Sritalapat P. Post-buckling behavior illustrated by two-DOF model. J Eng Mech 1988;114(2):314–27.
[19] Antman SS, Marlow RS. New phenomena in the buckling of arches described by refined theories. Int J Solids Struct 1993;30:2213–41.
[20] Bochenek B. Problems of structural optimization for post-buckling behavior. Struct Multidiscip Optim 2003;25:423–35.
[21] Namita Y. Die Theorie II. Ordnung von krummen Stablen und ihre Anwendung auf das Kipp-Problem des Bogentragers. J Jpn Soc Civ Eng 1968;155:32–41.
[22] Levy M, Salvadori M. Why buildings fall down – how structures fail. Scranton: W. W. Norton & Company Incorporated; 1992.
[23] EN 1993-1-1: general rules and rules for buildings. CEN European Committee for Standardization, Bruxelles, Belgium; 1993.
[24] EN 1993-1-7: general rules – strength and stability of planar plated structures subject to out of plane loading. CEN European Committee for Standardization, Bruxelles, Belgium; 1993.
[25] Ziemian DR. Guide to stability design criteria for metal structures. sixth ed. John Wiley and Sons; 2010.